Talanta 98 (2012) 241–246

Contents lists available at SciVerse ScienceDirect

Talanta

journal homepage: www.elsevier.com/locate/talanta

On-line measurement of propofol using membrane inlet ion mobility spectrometer

Qinghua Zhou [a,b], Weiguo Wang [a], Huaiwen Cang [a], Yongzhai Du [a,b], Fenglei Han [a,b], Chuang Chen [a,b], Shasha Cheng [a,b], Jinghua Li [a], Haiyang Li [a,*,1]

[a] Dalian Institute of Chemical Physics, Chinese Academy of Sciences, Dalian, Liaoning 116023, PR China
[b] Graduate University of Chinese Academy of Sciences, Beijing 100049, PR China

ARTICLE INFO

Article history:
Received 14 April 2012
Received in revised form
29 June 2012
Accepted 1 July 2012
Available online 10 July 2012

Keywords:
Membrane inlet
Ion mobility spectrometer
Propofol
Exhaled air

ABSTRACT

The concentration of propofol in patient's exhaled air is an indicator of the anesthetic depth. In the present study, a membrane inlet ion mobility spectrometer (MI-IMS) was built for the on-line measurement of propofol. Compared with the direct sample introduction, the membrane inlet could eliminate the interference of moisture and improve the selectivity of propofol. Effects of membrane temperature and carrier gas flow rate on the sensitivity and response time have been investigated experimentally and theoretically. Under the optimized experimental conditions of membrane temperature 100 °C and carrier gas flow rate 200 mL min^{-1}, the calculated limit of detection (LOD) for propofol was 1 ppbv, and the calibration curve was linear in the range of 10–83 ppbv with a correlation coefficient (R^2) of 0.993. Finally, the propofol concentration in an anaesthetized mouse exhaled air was monitored continuously to demonstrate the capability of MI-IMS in the on-line measurement of propofol in real samples.

1. Introduction

Propofol is used as an intravenous anesthetic, and the concentration in serum is important for anesthetists to ensure patient safety and adjust the anesthetic depth appropriately. However, due to the complexity of blood samples, the measurement of serum propofol concentrations is off-line and time-consuming. Fortunately, in several studies, a close relation of propofol concentrations in exhaled air and that in serum was found [1,2], indicating that it was viable to measure the serum propofol concentration by analysis of exhaled air. Among these, Takita et al. and Harrison et al. accomplished the on-line measurement of propofol in patient's exhaled air by proton transfer reaction mass spectrometry (PTR-MS) [2,3]. In addition, methods such as selected ion flow tube mass spectrometry (SIFT-MS) [4], ion–molecule reaction mass spectrometry (IMR-MS) [5] and gas chromatography mass spectrometry (GC–MS) [6] also have been applied to measure the propofol in exhaled air. However, the instruments involved were expensive and bulky, hence they were not suitable for routine clinical use.

In contrast, the ion mobility spectrometer (IMS) thechnique has a large potential for monitoring compounds, including explosives [7,8], illegal drugs [9,10], and chemical warfare gents [11,12] due to the advantages of being relatively inexpensive, less bulky, and portable. Recently IMS has been applied in the analysis of exhaled air [13–17]. However, the moisture in exhaled air would interfere with the performance of the IMS, such as reducing the selectivity as well as the sensitivity [18,19]. An IMS in combination with a multicapillary column (MCC) was used to measure the propofol concentration in patient's exhaled air by Perl et al. and Carstens et al. [16,17]. Due to the pre-separation by the MCC, even though the relative humidity of patient's exhaled air was up to 100% and the matix of that was complex, the propofol in exhaled air was able to be identified and quantified. However, for the MCC, the diameter, length and film thickness of each column should meet stringent requirements [20]. Moreover, the use of MCC may cost a certain analysis speed.

In recent years, the membrane inlet technique has proved to be an effective method to eliminate moisture for detecting the volatile organic compounds (VOCs) by IMS [21–23]. Among these, the commonly used membrane is silicone membrane, a hydrophobic one that can resist the water vapor transmission through it. Furthermore, the solubilities, diffusivities, and permeabilities of analytes in the silicone membrane are determined by their chemical natures [24], therefore in some cases, the use of membrane inlet allows the IMS to boost the selectivity of

* Corresponding author. Tel.: +86 411 84379509; fax: +86 411 84379517.
E-mail address: hli@dicp.ac.cn (H. Li).
[1] Postal address: Group 102, 457 Zhongshan Road, Dalian, Liaoning 116023, China.

0039-9140/$ - see front matter © 2012 Elsevier B.V. All rights reserved.
http://dx.doi.org/10.1016/j.talanta.2012.07.001

analytes. Based on these characteristics of silicone membrane, the membrane-inlet would be a suitable sample introduction method for IMS to analyze the exhaled air. In this study, a membrane inlet ion mobility spectrometer (MI-IMS) was constructed and optimized for on-line measurement of propofol. The experimental parameters such as membrane temperature and carrier gas flow rate were optimized. The limit of detection, calibration curve and repeatability were investigated. Finally, the MI-IMS was applied to the mouse exhaled air sample.

2. Experimental

2.1. Instrumentation

The ion mobility spectrometer used in the experiment was built in our laboratory, which consisted of a radioactive ^{63}Ni ion source, a Bradbury–Nielsen (BN) gate, a drift region, an aperture grid, a Faraday plate and an amplifier, as shown in Fig. 1. The analyte was ionized in the ionization chamber, and then these ions were injected into the drift region by the BN gate, followed by the separation in a uniform electrical field. Air dried by molecular sieves and activated charcoals was divided into two streams via flow controllers (Beijing Sevenstar Electronics Co., Ltd., China, model D07-7B). One stream was sent into the permeate side of the membrane as the IMS carrier gas while the other stream was used as the IMS drift gas. The IMS was temperature-controlled with a tape heater, and the operating conditions are listed in Table 1.

The membrane inlet in Fig. 1 was constructed from stainless steel. A sheet silicone membrane (Technical Products INC. of GA, USA) was clamped in the membrane inlet. The thickness of the membrane was 50 μm, and its area exposed to sample gas was about 3 cm^2. Sample gas flowed along the feed side of the membrane continuously via a pump, so that the analytes permeated through the membrane layer and were sent into the IMS by the carrier gas. The membrane inlet was temperature-controlled with a rod heater and thermal resistor. In addition, the insulating material was wrapped around the membrane inlet to keep a constant temperature.

2.2. Treatment of membrane sheet

The commercial silicone membrane sheet typically contained some filler compounds, so it was cleaned with methanol in an ultrasonic bath for 20 min, before it was clamped in the membrane inlet kept at 150 °C. In the latter procedure, the membrane was flushed with clean dry carrier gas until only the reaction ion peak (RIP) persisted in the IMS spectrum.

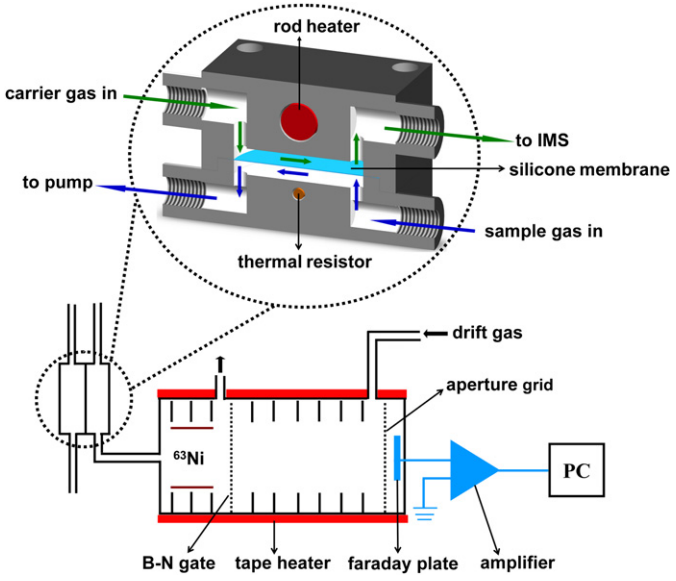

Fig. 1. Schematic drawing of the membrane inlet ion mobility spectrometer.

Table 1
Operating conditions for IMS.

Operating condition	Setting
Ionization source	^{63}Ni
Operating mode	Negative
Temperature of IMS	90 °C
Effect length of the drift region	6.5 cm
Drift field	380 V cm^{-1}
BN gate opening time	200 μs
Drift gas flow rate	350 mL min^{-1}

2.3. Chemicals

Methanol (≥ 99.9%) was purchased from Tianjin Kermel Chemical Reagent Co., Ltd. (Tianjin, China). Propofol was purchased from J&K Scientific Ltd. (Beijing, China). Propofol injection was purchased from Xi'an Pharmaceutical, Ltd. (Xi'an, China). A mouse was provided by Dalian Medical University, China.

2.4. Transport model of propofol across the silicone membrane

Based on the transport model of VOCs across the silicone membrane [24], for an unit exposed membrane area, the cumulative volume of propofol in the carrier gas $Q(t)$ (cm^3) can be described as follows:

$$Q(t)=\frac{DC_1t}{l}-\frac{lC_1}{6}-\frac{2lC_1}{\pi^2}\sum_{n=1}^{\infty}\frac{(-1)^n}{n^2}\exp\left(\frac{-Dn^2\pi^2t}{l^2}\right) \quad (1)$$

where D is the diffusivity of propofol in the silicone membrane (cm^2 s^{-1}), C_1 is the propofol concentration on the feed side surface of the membrane (cm^3 cm^{-3}), l is the thickness of the silicone membrane (cm), and t is the time (s). Considering the carrier gas flow rate, the propofol concentration in the carrier gas can be described as following:

$$C_A(t)=\frac{dQ(t)}{dt}\frac{1}{V}=\frac{DC_1}{lV}\left[1+2\sum_{n=1}^{\infty}(-1)^n\exp\left(\frac{-Dn^2\pi^2t}{l^2}\right)\right] \quad (2)$$

where $C_A(t)$ is the propofol concentration in the carrier gas (cm^3 cm^{-3}), V is the carrier gas flow rate (cm^3 s^{-1}). As the velocity of molecular diffusion across the silicone membrane is affected by the carrier gas flow rate [25], a factor "γ " is used to revise Eq. (2), yielding the following equation:

$$C_A(t)=\frac{DC_1}{lV}\left[1+2\sum_{n=1}^{\infty}(-1)^n\exp\left(\frac{-\gamma Dn^2\pi^2t}{l^2}\right)\right] \quad (3)$$

According to Henry's law:

$$C_1=SP_A \quad (4)$$

where S is the solubility of propofol in the silicone membrane (cm^3 cm^{-3} cm^{-1} Hg), and P_A is the partial pressure of propofol vapor in the sample gas (cm Hg). Substituting Eq. (4) into Eq. (3) yields

$$C_A(t)=\frac{KP_A}{lV}\left[1+2\sum_{n=1}^{\infty}(-1)^n\exp\left(\frac{-\gamma Dn^2\pi^2t}{l^2}\right)\right] \quad (5)$$

where $K=DS$, defined as the permeability of propofol in the silicone membrane (cm^3 cm^{-3} cm^{-2} s^{-1} cm^{-1} Hg), is a product of solubility and diffusivity.

In the present study, the diffusivity of propofol in the silicone membrane was determined by fitting the experimental data using this model. Furthermore, this model was used to explain the effects of experimental parameters.

3. Results and discussions

3.1. Dehumidification capacity of the silicone membrane

To investigate the dehumidification capacity of the silicone membrane for humid samples, a humidity resistance test was performed. In this test, five air sample gases, with the relative humidity (RH) of 0%, 39%, 58%, 74%, 98%, were sent into the feed side of the membrane. It was found that the RH of each outflow was below 1% when the RH of carrier gas was kept as 0%, which ensured that the RIP peaks did not drift with the RH variation of the sample gas. Thus, by the use of silicone membrane the negative effects of moisture in exhaled air on the IMS was avoided.

3.2. Selectivity of the silicone membrane

To investigate the selectivity of the silicone membrane for propofol, direct sample introduction and membrane inlet sample introduction were performed. The IMS spectra of the background, mouse exhaled air, and propofol in the mouse exhaled air are compared in Fig. 2. With the direct sample introduction, sample gases were directly sent into the IMS by the carrier gas. Comparing the IMS spectrum of the background (Fig. 2(a)) with that of the mouse exhaled air (Fig. 2(b)), it indicates that the RIP has shifted from 5.20 ms to about 5.56 ms due to the high humidity of the mouse exhaled air. Furthermore, two unidentified ion peaks at 6.32 ms and 7.48 ms appeared in Fig. 2(b), which were probably attributed to the matrix of the mouse exhaled air. When mixing the mouse exhaled air with propofol, an unresolved propofol ion peak was detected at 8.72 ms, as shown in Fig. 2(c).

However, with the membrane inlet sample introduction, the positions of RIP were not affected by the high humidity of the mouse exhaled air, according to the comparison of IMS spectra of the background (Fig. 2(d)) and mouse exhaled air (Fig. 2(e)). In addition, except the RIP, no other ion peaks were found in the IMS spectrum of the mouse exhaled air (Fig. 2(e)). Furthermore, when mixing the mouse exhaled air with propofol, a separated propofol ion peak was detected at 8.64 ms, as depicted in Fig. 2(f), suggesting that propofol in the mouse exhaled air could selectively permeate through the membrane.

3.3. Effects of membrane temperature

Since the permeability (K) and diffusivity (D) of propofol in the silicone membrane depend on the temperature, according to Eq. (5), the membrane temperature may influence the sensitivity and response time. The peak intensity of 25 ppbv propofol was monitored as a function of time at different temperatures, as shown in Fig. 3(a). The peak intensity rose quickly at the beginning, and then reached a constant value (defined as I_{steady}).

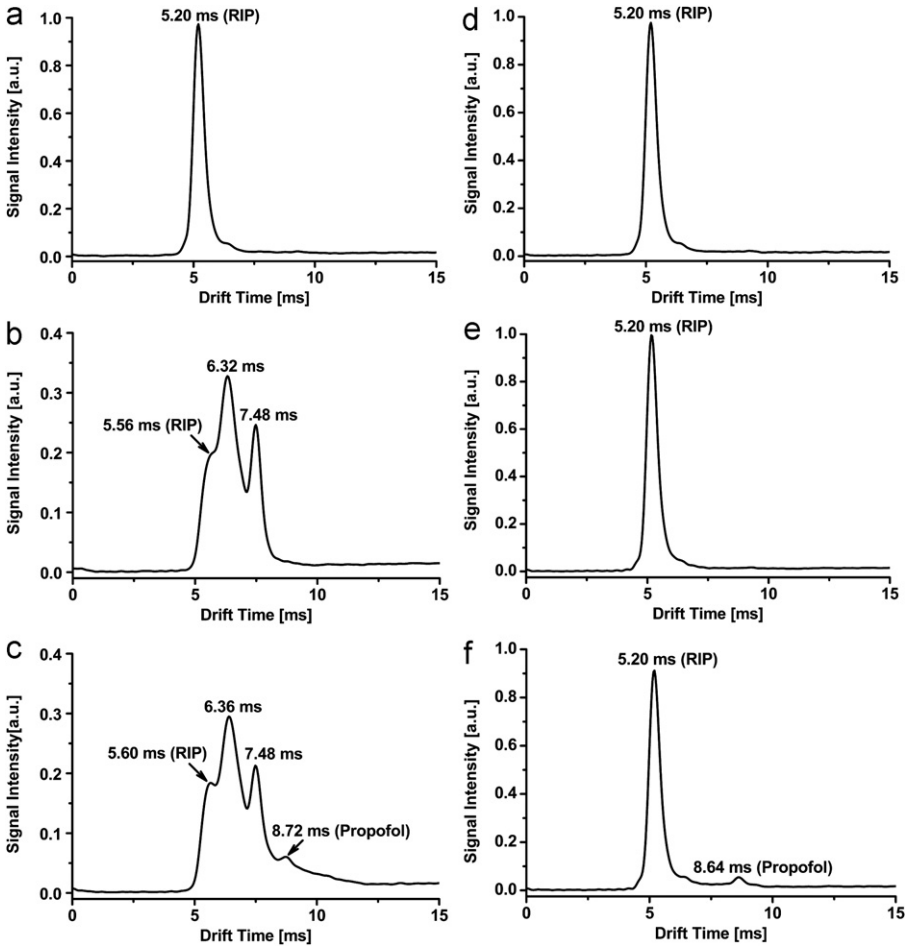

Fig. 2. IMS spectra of (a) background, (b) mouse exhaled air, (c) propofol in mouse exhaled air with the direct sample introduction; IMS spectra of (d) background, (e) mouse exhaled air, (f) propofol in mouse exhaled air with the membrane inlet sample introduction.

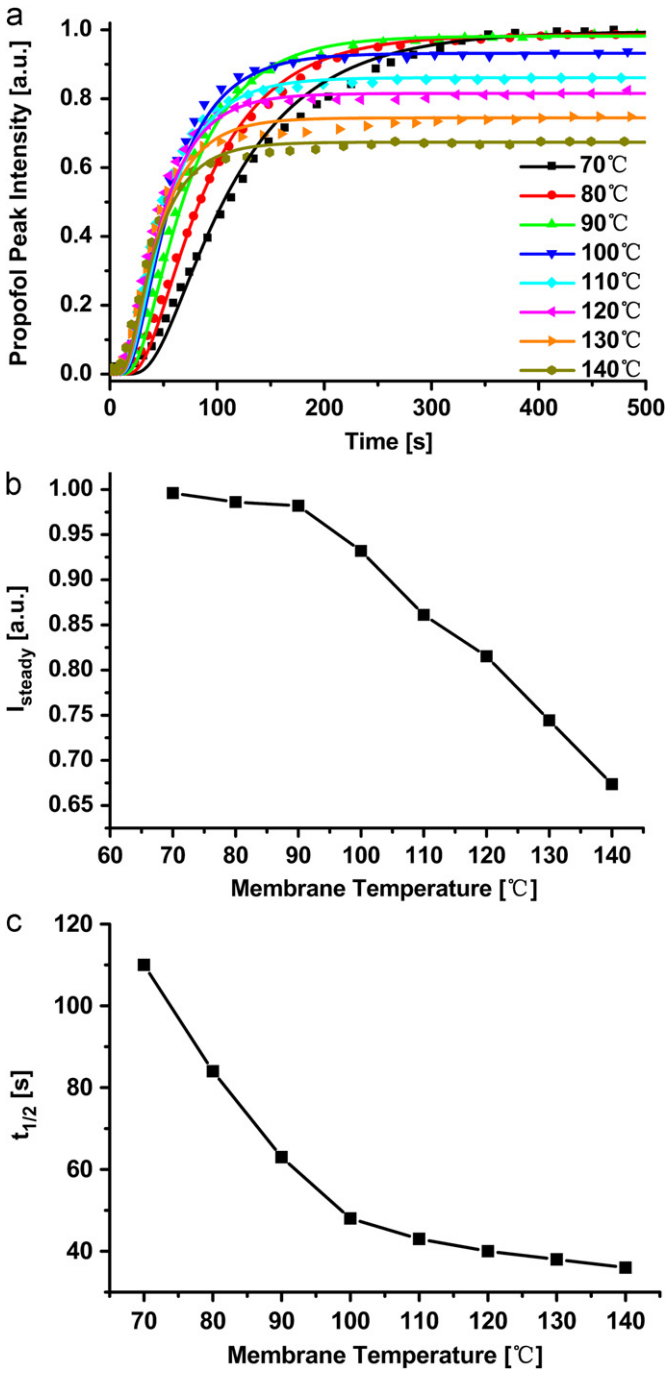

Fig. 3. (a) Propofol peak intensity as a function of time at different membrane temperatures. The symbols are experimental data, and the lines are fitted results based on the transport model; (b) effect of membrane temperature on I_{steady}; (c) effect of membrane temperature on $t_{1/2}$.

The dependence of I_{steady} on the membrane temperature is shown in Fig. 3(b). With an increase of the membrane temperature from 70 to 140 °C, the I_{steady} was decreased, suggesting that the propofol concentration in the carrier gas at steady-state permeation (defined as C_{steady}) was reduced. In Eq.(5), when $t \to \infty$, the permeation of propofol in the silicone membrane achieved the steady state, so C_{steady} can be described as $C_{steady} = (KP_A)/(lV)$, indicating that C_{steady} was proportional to the permeability of propofol in the silicone membrane. On the right hand side of this equation, only the permeability K was the function of temperature, therefore, this variation in C_{steady} was mainly attributed to a lower permeability of propofol in the silicone membrane under a higher membrane temperature.

Furthermore, higher membrane temperatures resulted in increased diffusivities and therefore faster response times. It was convenient to relate the response time to the time required to achieve 50% steady-state permeation (defined as $t_{1/2}$), thus, the $t_{1/2}$ values at different membrane temperatures were determined in Fig. 3(c). As expected, increasing the membrane temperature from 70 to 140 °C brought an approximately 70% decrease in $t_{1/2}$. In order to shorten the $t_{1/2}$ value on the basis of an acceptable I_{steady}, a membrane temperature of 100 °C was chosen as the optimized condition.

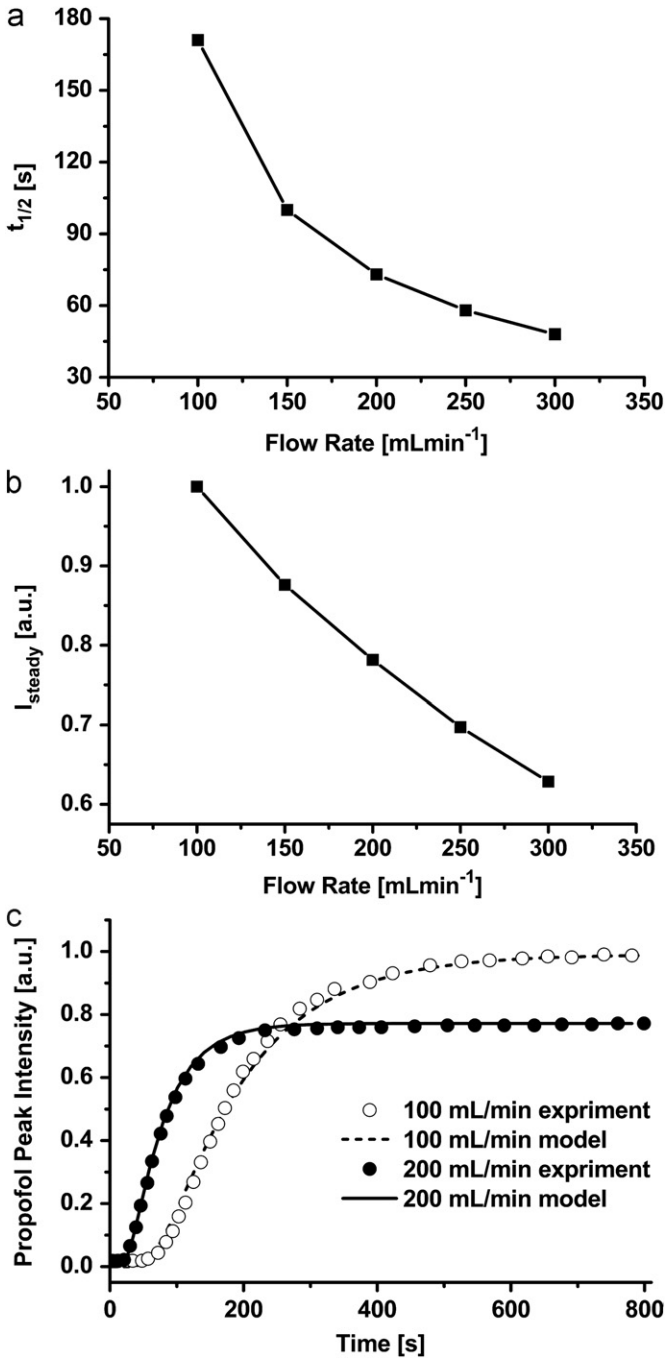

Fig. 4. (a) Effect of carrier gas flow rate on $t_{1/2}$; (b) effect of carrier gas flow rate on I_{steady}; (c) comparison of experimental data and calculated results for carrier gas flow rates of 100 and 200 mL min^{-1}.

3.4. Effects of carrier gas flow rate

At a membrane temperature of 100 °C, the $t_{1/2}$ values collected at various carrier gas flow rates (from 100 to 300 mL min^{-1}) are shown in Fig. 4(a). It was clear that increased carrier gas flow rates led to a decrease of $t_{1/2}$, which was attributed to a higher Reynolds number. As the Reynolds number was increased, the mass transfer boundary layer resistance was reduced. In addition, the temperature at the membrane surface and in the carrier gas was almost the same, resulting in a reduction of the thermal boundary layer resistance [26]. Therefore, an increase in carrier gas flow rate would enhance the permeation of propofol in silicone membrane. However, the propofol desorbing from the permeate side of the membrane would be diluted by the carrier gas. As shown in Fig. 4(b), the higher the carrier gas flow rate, the lower the I_{steady}. Thus, restricted by both $t_{1/2}$ and I_{steady}, the carrier gas flow rate was chosen to be 200 mL min^{-1}.

To obtain the diffusivity of propofol in the silicone membrane, the experimental data originating at the carrier gas flow rate of 300 mL min^{-1} was best-fitted by Eq. (3), assuming $\gamma=1$. As a result, the diffusivity of propofol in the silicone membrane at 100 °C was fitted to be about 6.34×10^{-8} cm^2 s^{-1}. Using this fitted diffusivity, the experimental data for the flow rates of 100 and 200 mL min^{-1} was fitted by Eq. (3), with $\gamma=0.32$ and 0.80 respectively. In Fig. 4(c), the experimental time profiles of propofol peak intensity for the two flow rates are plotted as symbols, while the calculated results based on Eq. (3) for the two flow rates are plotted as lines. Both of the experimental data and model prediction indicated that the model was able to fit the experimental data consistently.

3.5. Response of MI-IMS to the variation in propofol concentration

As the permeation of propofol through the silicone membrane was a time dependent process, when the propofol concentration in the feed side was changed, a certain time was required before new steady-state permeation was established. To investigate the response of MI-IMS to the variation in propofol concentration, a response time measurement was carried out by switching the propofol concentration in the sample gas as following: initially from 100 ppbv to 60 ppbv, and then from 60 ppbv to 100 ppbv, finally from 100 ppbv to 40 ppbv. The time profile of propofol peak intensity is shown in Fig. 5. In this experiment, once the propofol concentration was switched, a variation in the propofol peak intensity could be observed after about 30 s, and the time needed to achieve new steady-state permeation was 186 s, 200 s and 235 s. Thus, corresponding to a variation in propofol concentration within 60 ppbv, there was a response time less than 4 min.

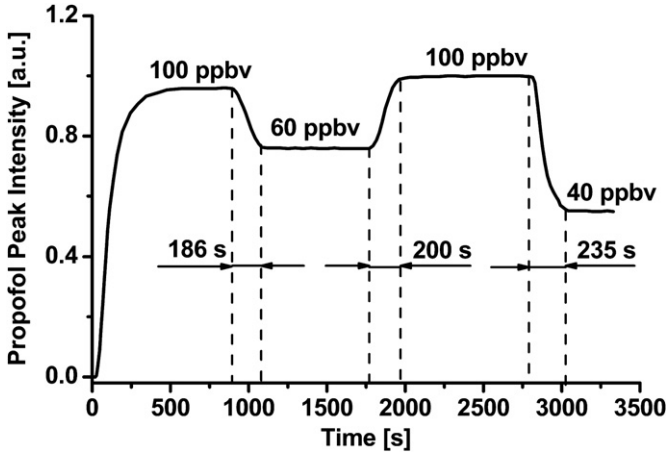

Fig. 5. Response of MI-IMS to the variation in propofol concentration.

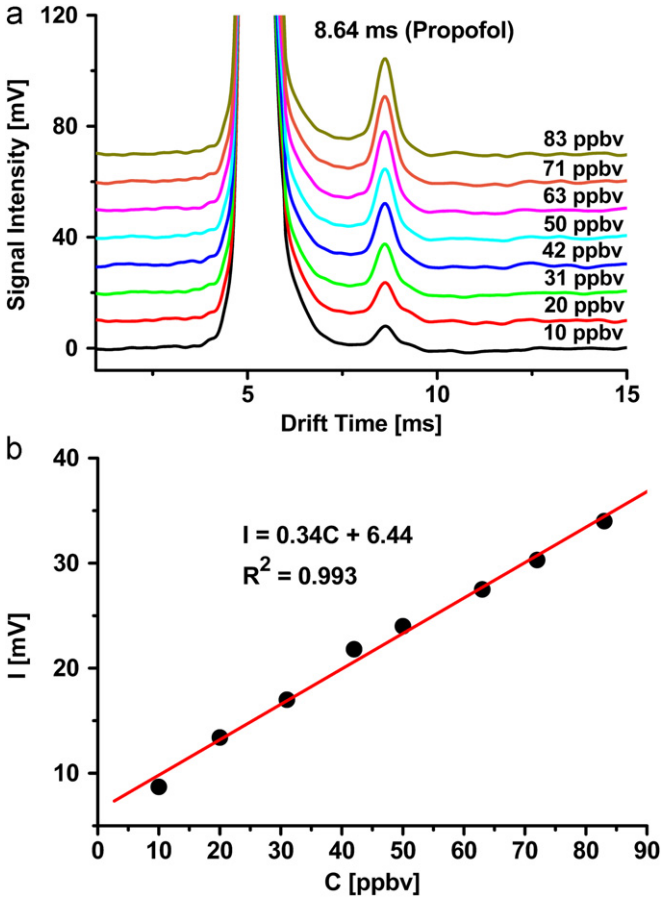

Fig. 6. (a) IMS spectra of 10–83 ppbv propofol at steady-state permeation; (b) calibration curve for propofol.

3.6. Quantification of propofol

Under the optimized conditions mentioned above, 10–83 ppbv propofol sample gases were measured by MI-IMS. The IMS spectra at steady-state permeation were collected and are depicted in Fig. 6(a). By plotting the propofol peak intensity (I) against the concentration (C), as seen in Fig. 6(b), the calibration curve for propofol was linear in the range of 10–83 ppbv with a correlation coefficient R^2 of 0.993. The peak intensity of 10 ppbv propofol was 10 times higher than 3σ variation of baseline, suggesting that the LOD for propofol was 1 ppbv. In addition, the repeatability was found to be satisfactory for the measurement of propofol by MI-IMS, with a relative standard deviation (RSD) of 2.7% for 5 times measurement of a 31 ppbv propofol sample gas.

3.7. Monitoring of propofol in the exhaled air of a mouse

A mouse intravenously injected with propofol injection was restricted in a glass container, and then the mouse exhaled air was continuously measured by MI-IMS. In Fig. 7, the time profile of propofol peak intensity shows that it needed about 10 min before the propofol signal could be observed. Due to the metabolism of propofol in the mouse body, the propofol concentration in the mouse exhaled air rose, giving an increase of propofol peak intensity. As the mouse was no longer injected with propofol, the propofol peak intensity reached a maximum at about 29 min, and then presented a decrease trend. In summary, MI-IMS enabled the

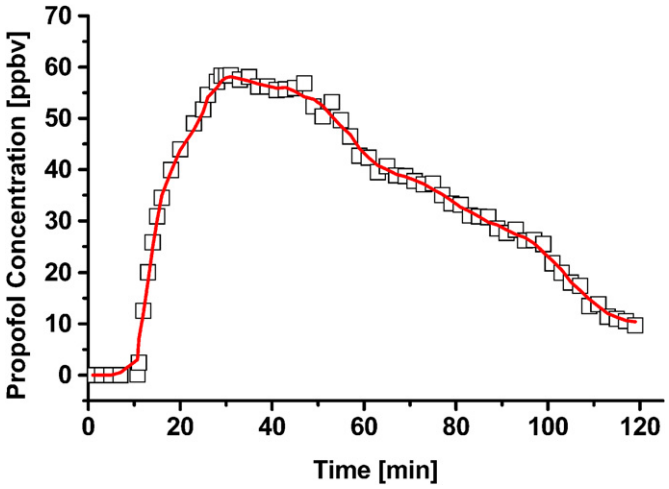

Fig. 7. Monitoring of propofol in the mouse exhaled air.

on-line and continuous monitoring of propofol in the mouse exhaled air, which could be readily extended to the human exhaled air.

4. Conclusion

This study demonstrates the capability of MI-IMS for the on-line measurement of propofol in exhaled air without sample pre-separation. Besides providing a direct and continuous sample introduction for IMS, the membrane inlet system furthermore eliminated the interference of high humidity and complex matrix in exhaled air. The effects of membrane temperature and carrier gas flow rate on the propofol measurement were both optimized. Under the optimized conditions for quantitative measurement, a calculated LOD of 1 ppbv can be obtained. Propofol in the mouse exhaled air was monitored as a simulated application, in which the variation of propofol concentration was observed easily. However, due to the permeation of propofol through the membrane, there was a certain response time of MI-IMS to the variation of propofol concentration. To shorten this response time, further studies should be conducted, for example, using a thinner membrane or improving the structure of membrane inlet. Furthermore, MI-IMS developed here can be similarly extended to monitor other VOCs in human breath for disease screening.

Acknowledgments

This work is partly supported by National High-Tech Research and Development Plan (No. 2011AA060602), Natural Science Foundation of China (Nos. 11004190, 20877074, 21077101).

References

[1] M. Grossherr, A. Hengstenberg, T. Meier, L. Dibbelt, K. Gerlach, H. Gehring, Anesthesiology 104 (2006) 786–790.
[2] A. Takita, K. Masui, T. Kazama, Anesthesiology 106 (2007) 659–664.
[3] G.R. Harrison, A.D.J. Critchley, C.A. Mayhew, J.M. Thompson, Br. J. Anaesth. 91 (2003) 797–799.
[4] P.R. Boshier, J.R. Cushnir, V. Mistry, A. Knaggs, P. Španěl, D. Smith, G.B. Hanna, Analyst 136 (2011) 3233–3237.
[5] C. Hornuss, S. Praun, J. Villinger, A. Dornauer, P. Moehnle, M. Dolch, E. Weninger, A. Chouker, C. Feil, J. Briegel, M. Thiel, G. Schelling, Anesthesiology 106 (2007) 665–674.
[6] M. Grossherr, A. Hengstenberg, T. Meier, L. Dibbelt, B.W. Igl, A. Ziegler, P. Schmucker, H. Gehring, Br. J. Anaesth. 102 (2009) 608–613.
[7] G.R. Asbury, J.r. Klasmeier, H.H. Hill, Talanta 50 (2000) 1291–1298.
[8] T. Khayamian, M. Tabrizchi, M.T. Jafari, Talanta 59 (2003) 327–333.
[9] T. Khayamian, M. Tabrizchi, M.T. Jafari, Talanta 69 (2006) 795–799.
[10] A.B. Kanu, H.H. Hill, Talanta 73 (2007) 692–699.
[11] A.B. Kanu, P.E. Haigh, H.H. Hill, Anal. Chim. Acta 553 (2005) 148–159.
[12] P. Rearden, P.B. Harrington, Anal. Chim. Acta 545 (2005) 13–20.
[13] V. Ruzsanyi, J.I. Baumbach, S. Sielemann, P. Litterst, M. Westhoff, L. Freitag, J. Chromatogr. A 1084 (2005) 145–151.
[14] J.I. Baumbach, J. Breath Res. 3 (2009) 034001.
[15] A. Bunkowski, B. Bödeker, S. Bader, M. Westhoff, P. Litterst, J.I. Baumbach, J. Breath Res. 3 (2009) 046001.
[16] T. Perl, E. Carstens, A. Hirn, M. Quintel, W. Vautz, J. Nolte, M. Junger, Br. J. Anaesth. 103 (2009) 822–827.
[17] E. Carstens, A. Hirn, M. Quintel, J. Nolte, M. Jünger, T. Perl, W. Vautz, Int. J. Ion Mobil. Spectrom. 13 (2010) 37–40.
[18] V. Bocos-Bintintan, A. Brittain, C.L.P. Thomas, Analyst 126 (2001) 1539–1544.
[19] M. Mäkinen, M. Sillanpää, A.-K. Viitanen, A. Knap, J.M. Mäkelä, J. Puton, Talanta 84 (2011) 116–121.
[20] M.v. Deursen, M.v. Lieshout, R. Derks, H.-G. Janssen, C. Cramers, J. High Resolut. Chromatogr. 22 (1999) 119–122.
[21] H. Borsdorf, A. Rämmler, J. Chromatogr. A 1072 (2005) 45–54.
[22] Y. Du, W. Zhang, W. Whitten, H. Li, D.B. Watson, J. Xu, Anal. Chem. 82 (2010) 4089–4096.
[23] C. Wan, P.d.B. Harrington, D.M. Davis, Talanta 46 (1998) 1169–1179.
[24] C.B. Almquist, S.-T. Hwang, J. Membr. Sci. 153 (1999) 57–69.
[25] W. Zhang, Y. Du, Z. Feng, J. Xu, Int. J. Ion Mobil. Spectrom. 13 (2010) 65–71.
[26] Z. Xie, T. Duong, M. Hoang, C. Nguyen, B. Bolto, Water Res. 43 (2009) 1693–1699.